The Astronomical Journal, 129:239–250, 2005 January

DISCOVERY OF A NEW LOW-LATITUDE MILKY WAY GLOBULAR CLUSTER USING GLIMPSE

Henry A. Kobulnicky,[1] A. J. Monson,[1] B. A. Buckalew,[1] J. M. Darnel,[1] B. Uzpen,[1] M. R. Meade,[2] B. L. Babler,[2] R. Indebetouw,[2] B. A. Whitney,[3] C. Watson,[2] E. Churchwell,[2] M. G. Wolfire,[4] M. J. Wolff,[3] D. P. Clemens,[5] R. Shah,[5] T. M. Bania,[5] R. A. Benjamin,[6] M. Cohen,[7] J. M. Dickey,[8] J. M. Jackson,[5] A. P. Marston,[9] J. S. Mathis,[4] E. P. Mercer,[6] J. R. Stauffer,[10] S. R. Stolovy,[10] J. P. Norris,[11] A. Kutyrev,[12] R. Canterna,[1] and M. J. Pierce[1]

Received 2004 August 25; accepted 2004 September 21

ABSTRACT

Spitzer Space Telescope imaging from the Galactic Legacy Infrared Mid-Plane Survey Extraordinaire (GLIMPSE) reveals a previously unidentified low-latitude rich star cluster near $l = 31.^{\circ}3$, $b = -0.^{\circ}1$. Near-infrared *JHK′* photometry from the Wyoming Infrared Observatory indicates an extinction of $A_V \simeq 15 \pm 3$ mag for cluster members. Analysis of ^{13}CO features along the same sight line suggests a probable kinematic distance of 3.1–5.2 kpc. The new cluster has an angular diameter of ~1–2 pc, a total magnitude corrected for extinction of $m_{K_0} = 2.1$, and a luminosity of $M_K \simeq -10.3$ at 3.1 kpc. In contrast to young massive Galactic clusters with ages less than 100 Myr, the new cluster has no significant radio emission. Comparison with theoretical *K*-band luminosity functions indicates an age of at least several gigayears and a mass of at least $10^5\ M_{\odot}$. Unlike known old open clusters, this new cluster lies in the inner Galaxy at $R_{GC} \simeq 6.1$ kpc. We designate this object "GLIMPSE-C01" and present evidence that it is a Milky Way globular cluster passing through the Galactic disk. We also identify a region of star formation and fan-shaped outflows from young stellar objects in the same field as the cluster. The cluster's passage through the Galactic molecular layer may have triggered this star formation activity.

Key words: galaxies: structure — Galaxy: stellar content — globular clusters: general — infrared: galaxies

Online material: color figures

1. INTRODUCTION

Infrared surveys of the Galactic plane, such as the Two Micron All Sky Survey (2MASS), have led to the discovery of several hundred new star clusters throughout the Milky Way disk (e.g., Borissova et al. 2003; Bica et al. 2003; Dutra et al. 2003; Hurt et al. 2000). Typically, clusters are identified by locating peaks in the surface density of stars using point-source catalogs. The majority of these clusters were previously undetectable in optical surveys because of high extinction at low latitudes. Near-infrared cluster searches, however, are still incomplete in the regions of highest extinction, where A_K may reach several magnitudes.

The Galactic Legacy Infrared Mid-Plane Survey Extraordinaire (GLIMPSE) is mapping the Galactic plane in four Infrared-Array Camera (IRAC; Fazio et al. 2004) bands at 3.6, 4.5, 5.8, and 8.0 μm from $|l| = 10^{\circ}$ to 65° and $|b| < 1^{\circ}$ (Benjamin et al. 2003). One of the primary science drivers for the survey is to make possible a complete census of star formation regions and stellar populations throughout the inner Galaxy, unhindered by extinction, at the same arcsecond angular resolutions as optical and near-IR surveys. The survey will also make possible the discovery of previously uncataloged stellar objects on the far side of the Galaxy or in highly obscured regions.

In this paper we report the serendipitous discovery of a rich star cluster in the first Galactic quadrant near $l = 31^{\circ}$, $b = -0.^{\circ}1$. The cluster may be a new member of the collection of ~150 (Harris 1996) Milky Way globular clusters. We refer to this object as GLIMPSE-C01.

2. DATA

2.1. *GLIMPSE Imaging and Photometry*

The segment of the Galactic plane from $l = 25^{\circ}$ to 40° was observed by the *Spitzer Space Telescope* with IRAC on 2004 April 21 as part of the GLIMPSE program. The total exposure time at each IRAC band is 2.4 s, and the instrumental resolution ranges from 1.″6 FWHM at 3.6 μm to 1.″9 FWHM at 8.0 μm. Mosaicked images of the $5' \times 5'$ IRAC frames were constructed by the GLIMPSE team using MONTAGE.[13] A member of the GLIMPSE team (A. J. M.) identified the cluster, which has no previous identification in the literature,

[1] Department of Physics and Astronomy, University of Wyoming, P.O. Box 3905, Laramie, WY 82072.
[2] Department of Astronomy, University of Wisconsin–Madison, 475 North Charter Street, Madison, WI 53706.
[3] Space Science Institute, Suite 205, 4750 Walnut Street, Boulder, CO 80301.
[4] Department of Astronomy, University of Maryland, College Park, MD 20742-2421.
[5] Institute for Astrophysical Research, Boston University, 725 Commonwealth Avenue, Boston, MA 02215.
[6] Department of Physics, University of Wisconsin–Whitewater, 800 West Main Street, Whitewater, WI 53190.
[7] Radio Astronomy Laboratory, 601 Campbell Hall, University of California, Berkeley, CA 94720.
[8] Department of Astronomy, University of Minnesota, 116 Church Street, SE, Minneapolis, MN 55455.
[9] ESTEC/SCI-SA, Postbus 299, NL-2200 AG Noordwijk, Netherlands.
[10] *Spitzer* Science Center, Mail Stop 314-6, California Institute of Technology, Pasadena, CA 91125.
[11] NASA Goddard Space Flight Center, LHEA, Code 661, Greenbelt, MD 20771.
[12] NASA Goddard Space Flight Center, SSAI, Code 685, Greenbelt, MD 20771.

[13] Montage software is funded by the National Aeronautics and Space Administration's Earth Science Technology Office.

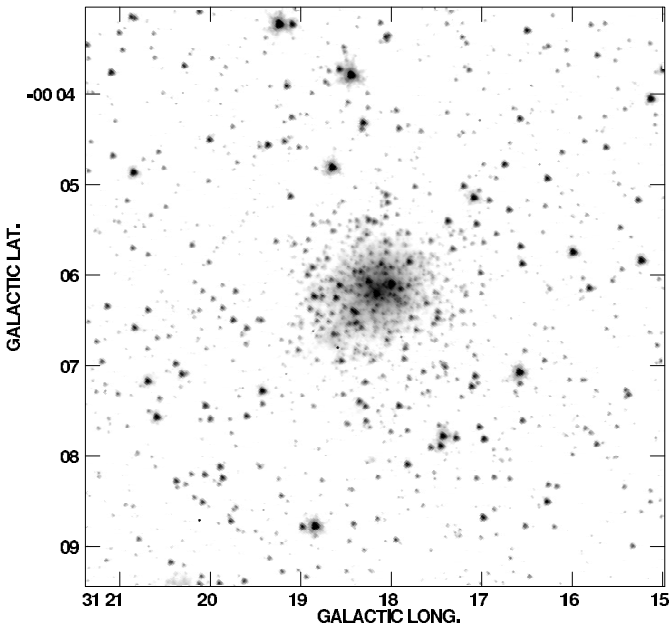

FIG. 1*a*

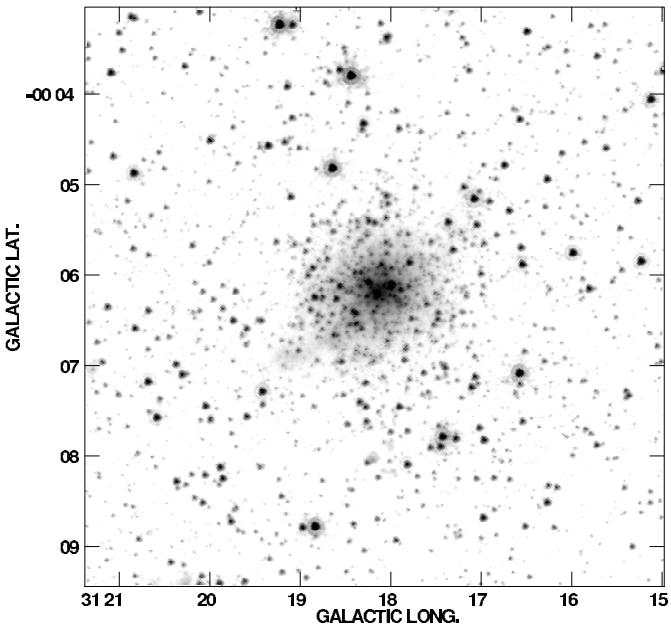

FIG. 1*b*

FIG. 1.—Logarithmic gray-scale images of the cluster at each of the four IRAC bandpasses: 3.6 μm (*a*), 4.5 μm (*b*), 5.8 μm (*c*), and 8.0 μm (*d*). The IRAC 1 and 2 bands ([*a*], [*b*]) are dominated by stellar photospheric emission. Stars become less prominent in IRAC bands 3 and 4, which are increasingly dominated by emission from known PAH bands.

during visual examination of the images. Inspection of initial 4.5 μm mosaicked images over the regions $l = 25^\circ-40^\circ$ and $l = 306^\circ-337^\circ$ shows that *no other similarly rich bright clusters are found in the 92 deg^2 of the plane surveyed to date.* The center of GLIMPSE-C01 is at $l = 31.^\circ30$, $b = -0.^\circ10$, or R.A. (J2000) = $18^h48^m49^s.7$, decl. (J2000) = $-01^\circ29'50''$. For further details on GLIMPSE imaging and photometry, see Mercer et al. (2004), Churchwell et al. (2004), Whitney et al. (2004), or Indebetouw et al. (2005).

Figure 1 shows logarithmic gray-scale representations of images in each of the four IRAC bands. The IRAC1 and IRAC2 bands ([*a*], [*b*]) are dominated by stellar photospheric emission from normal main-sequence stars. The cluster is the most prominent feature in the field. It subtends more than 2′ on the sky and is dominated by three bright pointlike sources, which we show to be multiple blended stars. We note that the brightest probable members are located near the cluster center, suggesting an age old enough for significant dynamical evolution to have occurred. Stars become less prominent in IRAC bands 3 and 4, which are increasingly dominated by emission from known polycyclic aromatic hydrocarbon (PAH) bands. Figures 1*c* and 1*d* reveal a bright swath (hereafter the "plume") of diffuse emission extending $\sim$1′ toward the Galactic south and toward higher longitudes. These panels also show a region (hereafter the "ribbon") of lower surface brightness diffuse emission running several arcminutes from the cluster toward the Galactic north and toward lower longitudes.

Figure 2 is a three-color image of GLIMPSE-C01 and the surrounding field constructed from the IRAC1 3.6 μm image (*blue*), the IRAC3 5.8 μm image (*green*), and the IRAC4 8.0 μm image (*red*). Contours indicate the 1420 GHz radio continuum emission in the NRAO VLA[14] Sky Survey (NVSS; Condon et al. 1998) archival image with contours at 2, 3, 4, 5, and 10 times the 1 σ rms noise of 1.3 mJy beam^{-1}. The cluster is coincident with a 3 σ radio detection at a level of 4.5 mJy per 45″ synthesized beam. Reduction of VLA B-configuration 1400 MHz archival data from program code AC629 (10″ synthesized beam) shows no point source at this location to a limit of 1.3 mJy, indicating that this radio emission in the NVSS is probably diffuse on scales larger than 10″. Several stronger (presumably unrelated) radio sources are visible to the Galactic south and toward lower longitudes from the cluster.

We note in Figure 2 the presence of several Y-shaped features 2′ south (Galactic) of the cluster. These objects appear similar to outflow cones from young stellar objects and probably indicate a region of star formation. In § 2.5 we show that this region is coincident with a peak in the ^{13}CO surface brightness at a velocity of 46 km s^{-1}, suggesting a kinematic distance of 3.1 kpc. It is not clear whether this star formation region is affiliated with the cluster or is a foreground or background object.

2.2. *WIRO Near-IR Imaging*

Near-infrared imaging of the GLIMPSE-C01 was obtained on 2004 July 31 using the 256^2 InSb Goddard Infrared Camera (GIRcam) on the 2.3 m Wyoming Infrared Observatory (WIRO) telescope. GIRcam has a pixel scale of 0.″46 pixel^{-1} at the Cassegrain focus. Seeing was 1.″1–1.″2. Images were obtained in the *J*, *H*, and *K*′ filters, with total exposure times of 120, 200, and 320 s, respectively, broken into multiple "dithered" exposures. Background images were obtained every 60 s on adjacent regions of sky. Data reduction followed standard procedures. Sky background exposures before and after each sequence were averaged and subtracted from each on-source image. Flat-field images in each filter were constructed from a median of at least 20 on-sky exposures obtained throughout the night. Cluster frames were registered and combined to produce final images. Conditions were photometric, and three standard stars from the list of Hawarden et al. (2001) covering a range of $J - K$ colors were observed for flux calibration. A collimation

[14] The Very Large Array is operated by the National Radio Astronomy Observatory, which is a facility of the National Science Foundation, operated under cooperative agreement by Associated Universities, Inc.

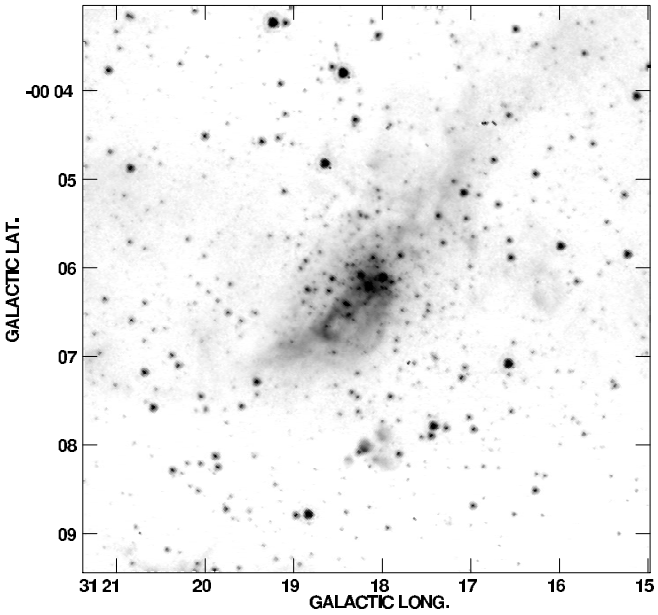

FIG. 1*c*

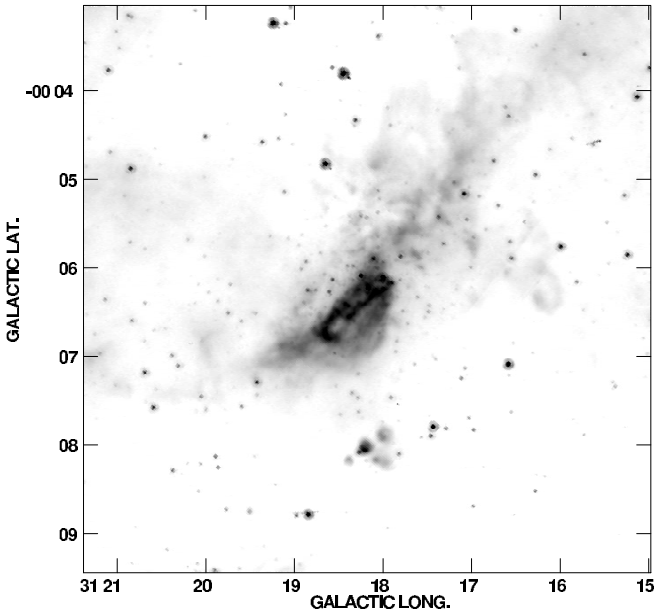

FIG. 1*d*

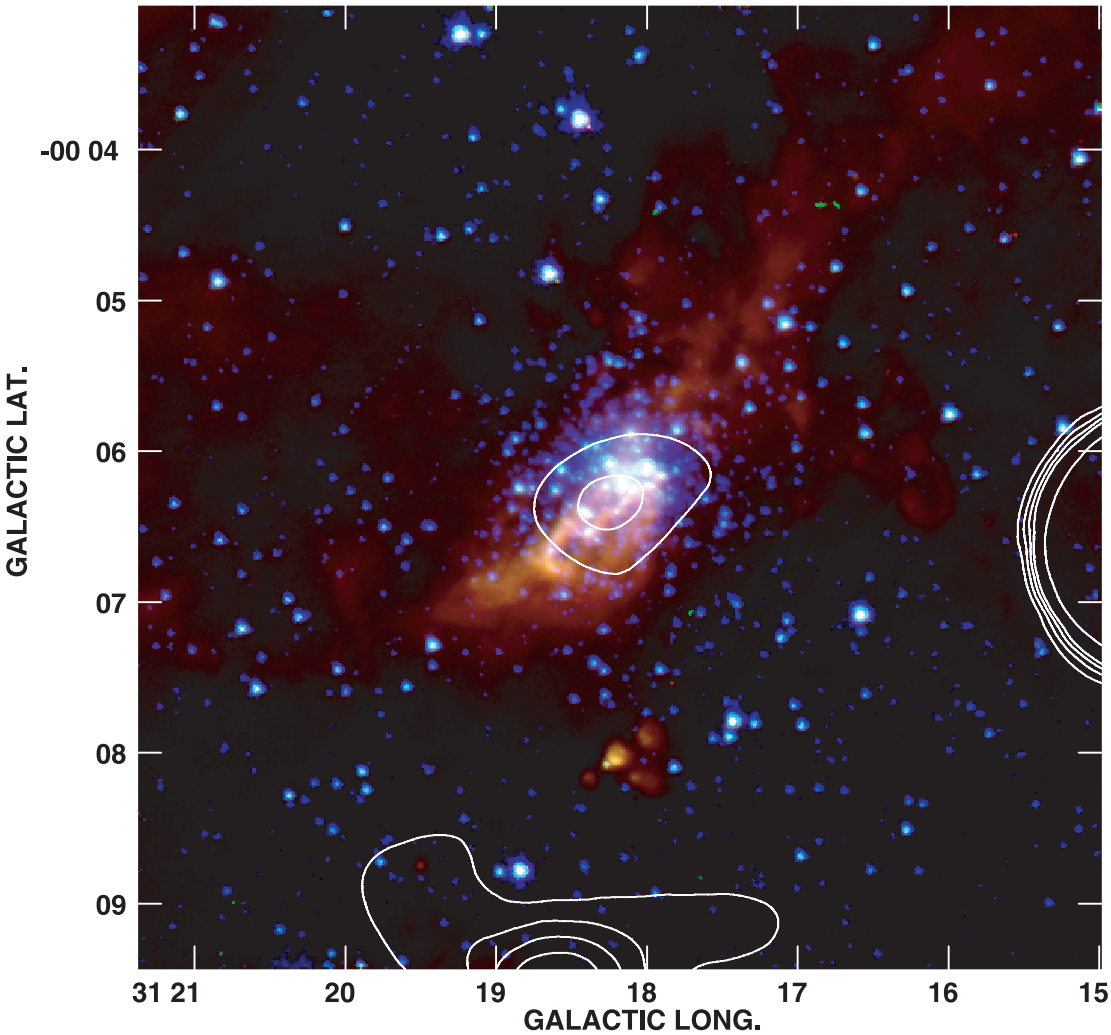

FIG. 2.—Three-color mid-infrared image of the cluster constructed from the IRAC 8.0 μm image (*red*), the IRAC 5.8 μm image (*green*), and the IRAC 3.6 μm image (*blue*). Contours show the 1420 GHz radio continuum emission from the NRAO VLA Sky Survey at multiples of 2, 3, 4, 5, and 10 times the 1 σ rms sensitivity of 1.3 mJy beam^{-1}. The marginal radio detection coincident with the cluster has a peak flux density of 4.5 mJy beam^{-1}.

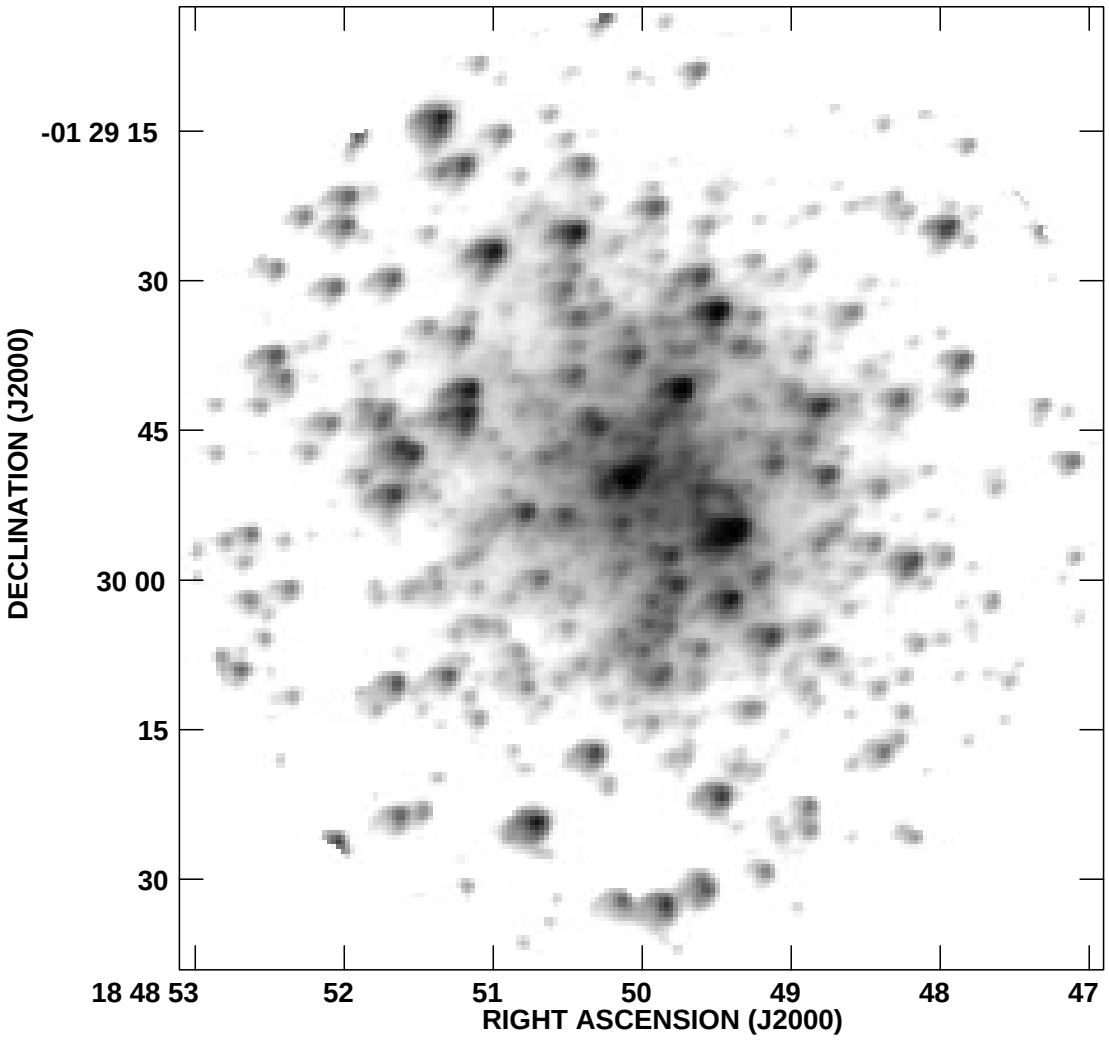

FIG. 3.—Logarithmic gray-scale representation showing the WIRO *H*-band image of GLIMPSE-C01.

problem with the secondary mirror produced stellar images with a narrow core (FWHM of 2.5 pixels, or 1.″15) but broad, asymmetric wings. Eighty-three percent of the power from a point source is contained in the core within a 4 pixel radius. DAOphot point-spread function (PSF)–fitting photometry was performed on the images to obtain *JHK′* photometry down to limiting magnitudes of 17.2, 15.5, and 14.5 in the *J*, *H*, and *K′* bands, respectively. In each filter four to five isolated stars were chosen to create a PSF profile, which was applied to the final images. Three deconvolution iterations were performed on the cluster to obtain magnitudes for 313 stars. The photometry is complete to a *K*-band magnitude of ~12.5. We transformed the *JHK′* magnitudes from the UKIRT photometric system to the 2MASS system using the relations of Carpenter (2001).

Figure 3 shows a WIRO *H*-band image of the cluster. Although the cluster is readily visible in 2MASS *J*, *H*, and *K′* images, it has not been previously identified in the literature. The WIRO data analyzed here have better sensitivity and angular resolution than the 2MASS archival images.

2.3. *Integrated Luminosity*

We measured the cluster's total flux by performing aperture photometry on the 2MASS *JHK′* images and our *Spitzer* IRAC1–IRAC4 images using a 90″ radius aperture and an annular background region from 90″ to 110″ from the cluster. Table 1 lists the integrated magnitudes and fluxes at each band. Note that the flux in IRAC bands 3 and 4 contains a considerable contribution from diffuse PAH emission (seen in Fig. 1), which is not present at other wavelengths.

2.4. *Far-Infrared IRAS*

An examination of archival images from the *IRAS* mission shows the new cluster to be located near the periphery of an extended region of diffuse far-infrared (FIR) emission. There is an *IRAS* source, IRAS 18462−0133, located within 20″ of the cluster's position. The *IRAS* flux densities, ranging from 16 Jy at 12 μm to 1500 Jy at 100 μm, appear in Table 1, although they are highly uncertain because of the large beam size in the high-background Galactic plane.

2.5. *Molecular Gas*

Millimeter-wave spectra from the ^{13}CO (1–0) Galactic Ring Survey (GRS; Simon et al. 2001; 46″ beam size) reveal strong emission at velocities near 46, 81, and 100 km s^{-1}. Figure 4 shows the ^{13}CO spectrum toward the cluster. The morphology of the molecular feature near 46 km s^{-1} is similar to that seen in the 8.0 μm PAH emission. Figure 5 shows the IRAC 3.6 μm (*blue*), 5.8 μm (*green*), and 8.0 μm (*red*) images with the zeroth moment GRS ^{13}CO map from 38 to 50 km s^{-1} in contours. Contour levels denote I_{CO} = 3.0, 3.5, 4.0, 4.5, 5.0,

TABLE 1
CLUSTER PARAMETERS

Parameter	Value
R.A. (J2000)	18 48 49.7
Decl. (J2000)	−01 29 50
l (deg)	31.30
b (deg)	−0.10
$R_\odot$ (kpc)[a]	3.1 ± 0.5
R_{GC} (kpc)[a]	6.8
r_h (arcsec)[b]	36
r_c (arcsec)[c]	30
m_K (mag)[d]	3.77 (19.3 Jy)
$J - H$ (mag)[d]	2.24
$J - K$ (mag)[d]	3.30
$F_{3.6}$ (Jy)[d]	14.3
$F_{4.5}$ (Jy)[d]	9.9
$F_{5.8}$ (Jy)[d,e]	14.6
$F_{8.0}$ (Jy)[d,e]	23.7
F_{12} (Jy)[f]	16.4L
F_{25} (Jy)[f]	18.9:
F_{60} (Jy)[f]	285
F_{100} (Jy)[f]	1516L
A_V (mag)	15 ± 3
A_K (mag)	1.7 ± 0.3
m_{K_0}[g]	2.07 ± 0.3
$V - K$[h]	1.5–1.9
M_K[i]	−10.3 ± 0.6
M_V[i, j]	−8.4 ± 3

NOTE.—Units of right ascension are hours, minutes, and seconds, and units of declination are degrees, arcminutes, and arcseconds. "L" denotes an upper limit on the flux listed in the *IRAS* Point Source Catalog.

[a] Estimated distance from the Sun and distance from the Galactic center.

[b] Half-light radius at K, 3.6 μm, and 4.5 μm.

[c] Core radius, defined as the radius where the surface brightness drops to half of the central value.

[d] Apparent magnitude or flux, not corrected for extinction, within a 90″ radius aperture.

[e] Note that the flux in IRAC bands 3 and 4 contains a considerable contribution from diffuse PAH emission that is not present at other wavelengths.

[f] *IRAS* flux; most measurements are highly uncertain because of large beam size and high background.

[g] Apparent magnitude, corrected for extinction, with $A_K = 1.7$ mag.

[h] Estimated $V - K$ color for starbursts of ages 10^8–10^9 yr (Starburst99) and for globular clusters (Harris 1996).

[i] Estimated absolute magnitudes at a distance of 3.1 kpc, including uncertainties on distance and reddening.

[j] Probable apparent integrated V magnitude given the adopted extinction and $V - K$ color.

5.5, 6.5, 7.0, and 7.5 K km s^{-1}. Assuming a ^{12}CO/^{13}CO ratio of 40 (Langer & Penzias 1990) and using $N_{H_2}(\mathrm{cm}^{-2}) = 2.0 \times 10^{20} I_{12_{CO}}$ (Maloney & Black 1988; Richardson & Wolfendale 1988), these contours correspond to molecular hydrogen columns of $2.5\text{–}6.0 \times 10^{22}$ cm^{-2}. The corresponding extinction associated with this molecular column density is $A_V = 15\text{–}32$ for the molecular component.[15] Note the CO peak, which coincides with the diffuse infrared (IR) clump 90″ directly south (in Galactic coordinates) of the cluster. This morphological correspondence is one of the features that demonstrates that the molecular emission is likely to be affiliated with the mid-IR PAH emission.

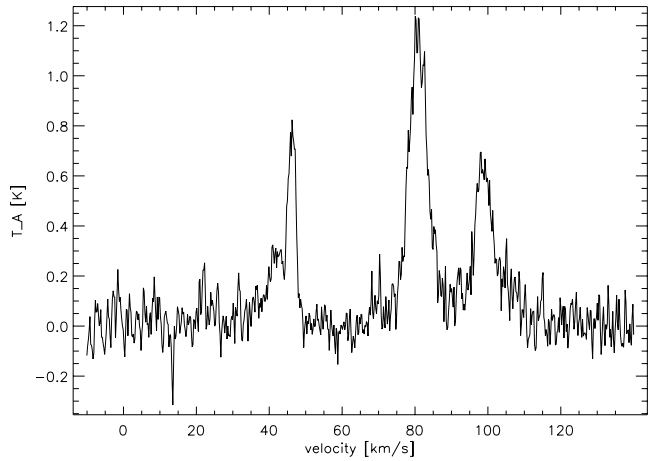

FIG. 4.—The ^{13}CO spectrum toward GLIMPSE-C01 from the Galactic Ring Survey (Simon et al. 2001). Strong emission features near 46, 81, and 100 km s^{-1} correspond to near/far kinematic distances of 3.1/11.4, 5.2/9.3, and 7.3 kpc, respectively.

3. ANALYSIS OF THE CLUSTER'S NATURE

3.1. *Extinction*

Figure 6 shows a $J - K$ versus $H - K$ color-color diagram of stars within 45″ of the cluster center. Lines indicate the loci of the main-sequence and giant branches for $A_V = 0$. Dots are field stars from the 2MASS point-source catalog within an annulus between 1′ and 9′ from the cluster. Large symbols are the 225 stars within 45″ of the cluster measured in our WIRO *JHK*′ photometry with photometric uncertainties less than 0.1 mag in all three bandpasses. The large star designates the integrated photometry of the cluster. An arrow shows the reddening vector for $A_V = 15$, which is equivalent to $A_K = 1.7$ using the extinction prescription of Cardelli et al. (1989). The dotted box denotes the region occupied by probable cluster members with similar colors.

Figure 6 shows that the vast majority of cluster stars are consistent with 12–18 mag of visual extinction, similar to that estimated from the CO column density in the 46 km s^{-1} feature. By comparison, field stars (*dots*) range from $A_V = 0$ to $A_V > 20$. The range of reddening among probable cluster members suggests patchy, variable extinction. We examined a reddening map of cluster stars and found no large-scale extinction gradient across the face of the cluster. Given the presence of dust emission features in the 8.0 μm image near the cluster, it is possible that dust mixed within the cluster produces the variation in extinction among members.

3.2. *Distance to the Cluster*

If the stellar cluster is located at the same distance as the mid-IR PAH emission, then the correspondence with the CO indicates a kinematic distance of either 3.1 or 11.5 kpc (Clemens 1985). However, even if the stellar cluster is not physically affiliated with the PAH emission, we can still constrain the distance to the cluster using the observed extinction ($A_V \simeq 15$ mag) and the kinematic distances of the ^{13}CO features. Given that the observed extinction is similar to that implied by the ^{13}CO column density in the 46 km s^{-1} feature alone, the cluster must be at least 3.1 kpc away. If the cluster were more distant than the 81

[15] Here we assume $A_V = 3.1E(B - V) = 3.1N_{H\,I}/5.8 \times 10^{21}$ (Bohlin et al. 1978). We convert the ^{13}CO column density to ^{12}CO column density assuming a ratio $^{12}\mathrm{CO}/^{13}\mathrm{CO} = 40$ and then use $N_{H\,I}$ (cm^{-2}) = N_{H_2} (cm^{-2}) = $2.0 \times 10^{22} I_{12_{CO}}$.

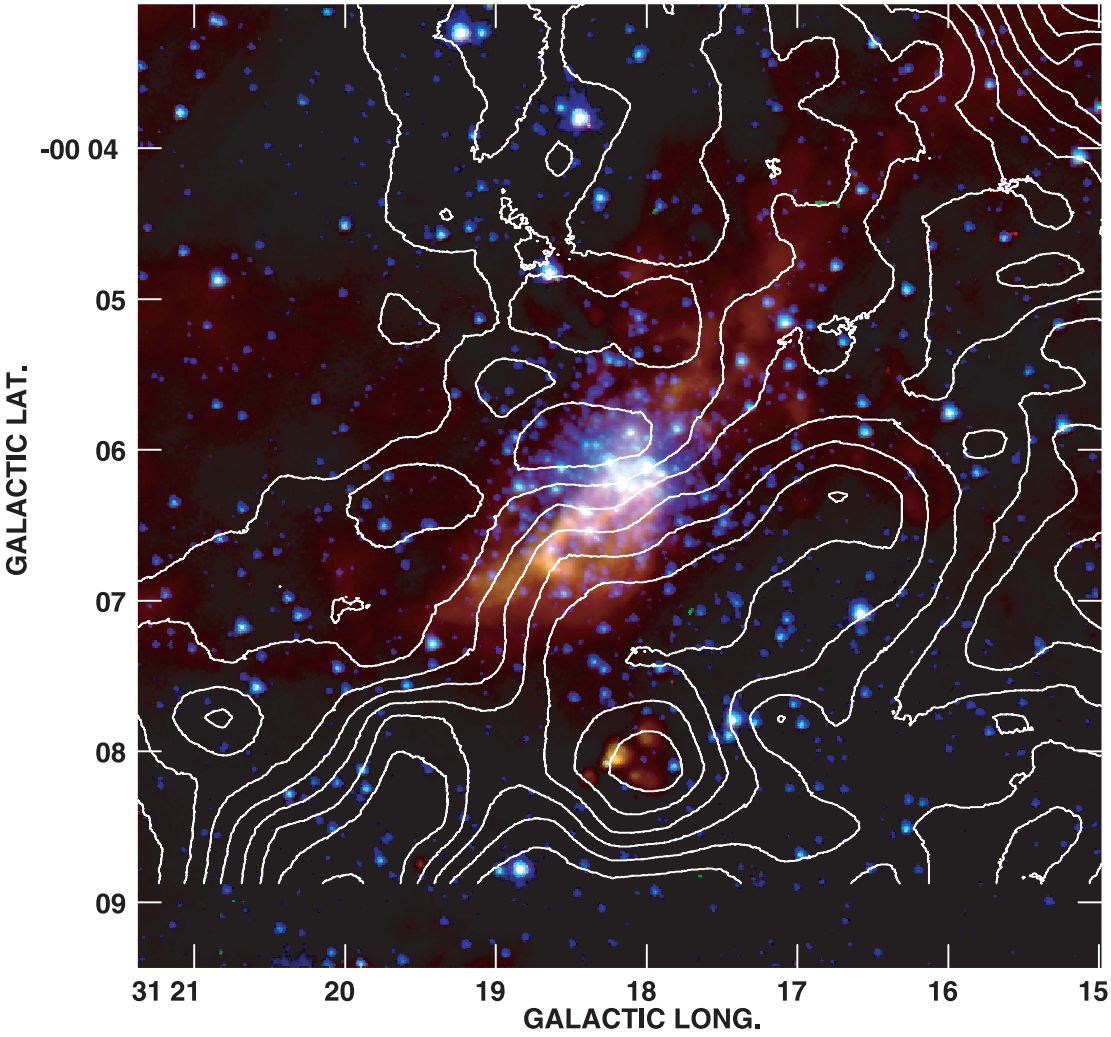

FIG. 5.—Three-color mid-infrared image of the cluster constructed from the IRAC 8.0 μm image (*red*), the IRAC 5.8 μm image (*green*) and the IRAC 3.6 μm image (*blue*). Contours show the ^{13}CO (1–0) molecular line emission from the Galactic Ring Survey (45″ beam size) integrated over the LSR velocity range 37–50 km s^{-1}. Contours denote levels of $I_{^{13}\mathrm{CO}} = 3.0$, 3.5, 4.0, 4.5, 5.0, 5.5, 6.5, 7.0, and 7.5 K km s^{-1}, which correspond to molecular hydrogen columns of $2.5-6.0\times10^{22}$ cm^{-2} (see text for details). The correspondence between diffuse PAH emission seen at 8.0 μm and ^{13}CO suggests a common origin and motivates adoption of the kinematic distance of 3.1 kpc.

or 100 km s^{-1} ^{13}CO features, then the integrated ^{13}CO column densities would produce extinctions of $A_V \gg 30$ mag, in contradiction to the observed $A_V \simeq 15$ mag. Thus, the cluster is on the *near* side of the clouds producing the 81 and 100 km s^{-1} emission. The kinematic distances of these features are 5.2/9.3 and 7.3 kpc (at the tangent point), respectively. Therefore, the cluster must be closer than 7.3 kpc and *may* be closer than 5.2 kpc, if the 81 km s^{-1} ^{13}CO feature is located at the near distance. The total extinction along this sight line estimated from *COBE* FIR maps is $A_V \simeq 80$ mag, corresponding to $A_K = 8.9$ (Schlegel et al. 1998). This is somewhat lower than the reddening estimate $A_V = 200$ based on the ^{13}CO intensity of $I_{^{13}\mathrm{CO}} = 23$ K km s^{-1} integrated over the entire Galactic velocity range. In either case, the extinction estimated from Figure 6 of $A_V \sim 15$ is significantly lower than these maximum values, suggesting that GLIMPSE-C01 is unlikely to be located on the far side of the Galaxy and most likely lies in the range 3.1–5.2 kpc.

3.3. *Color-Magnitude Diagram and K-Band Luminosity Function*

Figure 7 shows a K versus $J-K$ color-magnitude diagram (CMD) of cluster stars. Lines illustrate the solar metallicity isochrones of Bonatto et al. (2004) for ages of 10^8 yr (*solid*), 10^9 yr (*dotted*), and 10^{10} yr (*dashed*). All isochrones have been reddened by the equivalent of $A_V = 15$. Points are the stars within 45″of the cluster that are probable cluster members on the basis of color selection criteria (those contained within the dotted box in Fig. 6.) The top left, top right, and bottom left panels show the theoretical isochrones at distances suggested by the kinematics of the ^{13}CO features: 3.1, 5.2, and 9.3 kpc, respectively. At the two shorter distances, the tip of the 10^8 yr isochrone lies well above the magnitudes of the brightest cluster members, and the mean color is not well matched to the data. Both the 10^9 and 10^{10} yr isochrones provide reasonable fits to the colors and magnitudes of cluster stars at 3.1 and 5.2 kpc distances. For this most probable distance of 3.1 kpc, the data are consistent with an old cluster in excess of 1 Gyr. For the less probable distance of 5.2 kpc, illustrated in the top right panel of Figure 7, the 10^9 or 10^{10} yr isochrones are still in reasonable agreement with the data, while the 10^8 yr isochrone is still a poor fit. For the maximum possible distance of 9.3 kpc (*bottom left*) permitted by kinematic arguments, the tip of the 10^{10} yr isochrone lies below the brightest cluster members, while the 10^8 and 10^9 yr isochrones are now a reasonable fit both in color and K-band

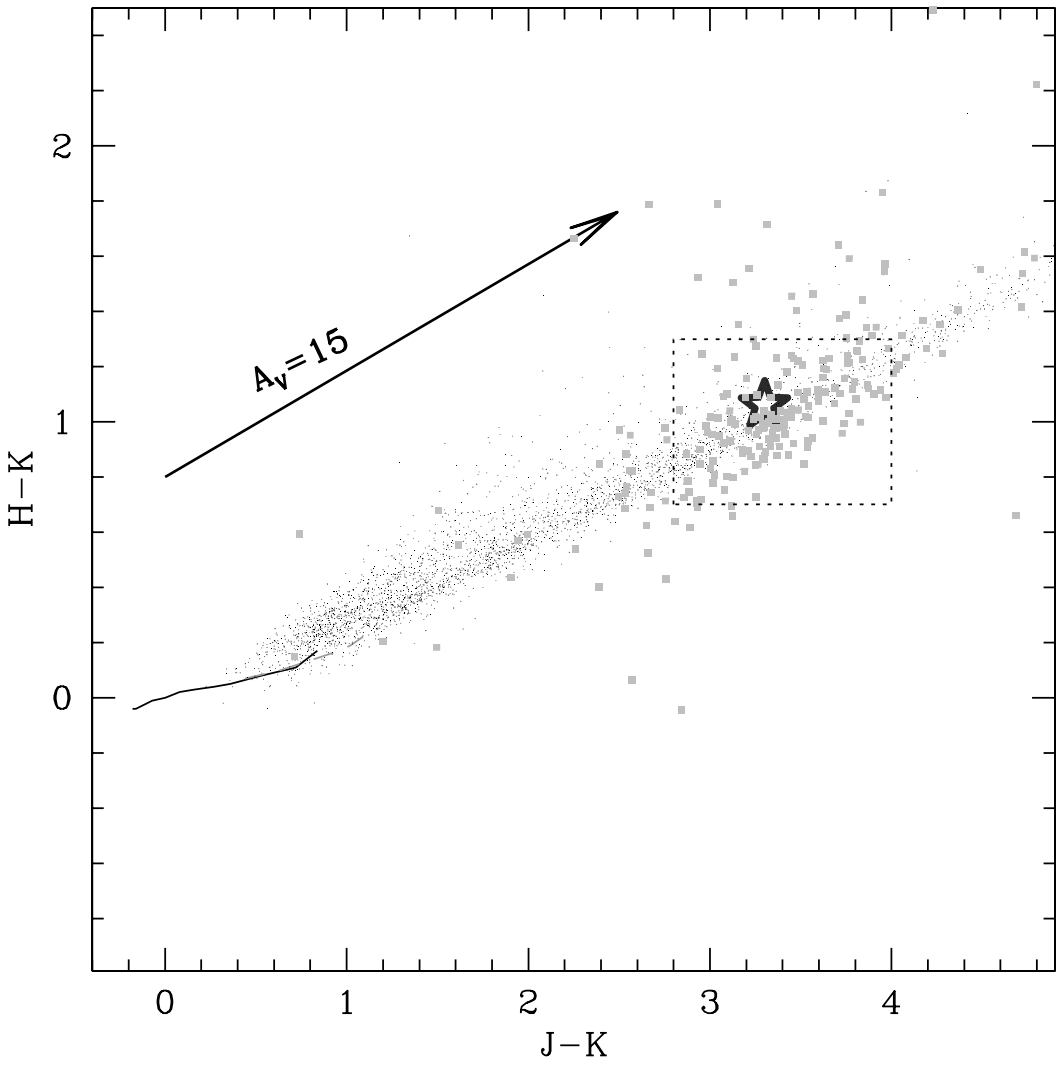

FIG. 6.—The *JHK′* color-color diagram of stars within 45″ of the cluster center. Lines show the loci of main-sequence and giant stars. Dots are field stars from the 2MASS catalog in an annulus between 1′ and 9′ from the cluster. Large points are stars within the 45″ of the cluster center, as measured with WIRO/GIRcam photometry. The star designates the integrated colors of the cluster. The arrow displays the reddening vector for $A_V = 15$. The dashed box encloses probable cluster members selected on the basis of similar reddening.

magnitude. Given the dispersion in color among cluster members, the strongest conclusion we can draw from Figure 7 is that either a nearby (3.1 kpc) old cluster or a more distant young cluster may be consistent with the data.

Figure 8 provides stronger constraints on the cluster age by showing the *K*-band luminosity function of the cluster (*thick line*) compared with expectations from the Bonatto et al. (2004) isochrones for a cluster mass of $10^5\ M_\odot$, a distance of 3.1 kpc, and three different ages. The *K*-band data have been corrected for 1.7 mag of extinction ($A_V = 15$). The top panel shows luminosity functions for $Z = 0.019$ (approximately solar metallicity) clusters with ages of 10^8, 10^9, and 10^{10} yr. The bottom panel shows luminosity functions for $Z = 0.001$ (approximately $\frac{1}{20}$ solar metallicity) clusters with ages of 3×10^9, 6×10^9, and 10^{10} yr. The histogram of the GLIMPSE-C01 luminosity function has been truncated at $K = 12.3$ ($M_K = -2.3$), where the cluster photometry becomes incomplete. Figure 8 shows that clusters of any metallicity with ages $\leq$3 Gyr are inconsistent with the observed luminosity function because of the lack of supergiants with luminosities $M_K < -6$ in GLIMPSE-C01. The best agreement between the models and data is for clusters with ages greater than 3 Gyr and masses from 10^5 to $3\times10^5\ M_\odot$, with the larger ages requiring larger masses. Figure 8 shows that a model with a mass of $3\times10^5\ M_\odot$ and an age of 10^{10} yr (*bottom*, *dashed line*) provides an excellent fit to the observed luminosity function. Such masses and ages are consistent with the canonical properties of globular clusters or extraordinarily old, massive, open clusters.

3.4. *Luminosity*

Using the measured total fluxes in Table 1, along with the reddening of $A_K = 1.7$ mag and distance estimates derived above, we estimate a total *K*-band luminosity of $M_K = -10.3 \pm 0.6$ for the cluster at the near 3.1 kpc distance. The corresponding *V*-band luminosity is $M_V = -8.4$, assuming $V - K = 1.9$, as appropriate for a 10^9 or 10^{10} yr old population (Leitherer et al. 1999). GLIMPSE-C01 is, therefore, much more luminous than Galactic open clusters (e.g., NGC 6791) and approaches the luminosity of the most massive globular clusters (Harris 1996). Adopting a greater distance would make GLIMPSE-C01 even more spectacular. At the maximal distance of 9.3 kpc, it would have $M_K = -12.8$ and $M_V = -10.9$ (assuming $V - K = 1.9$), making it more luminous than any known globular cluster. Such luminosities are typical of young (3–10 Myr) "super

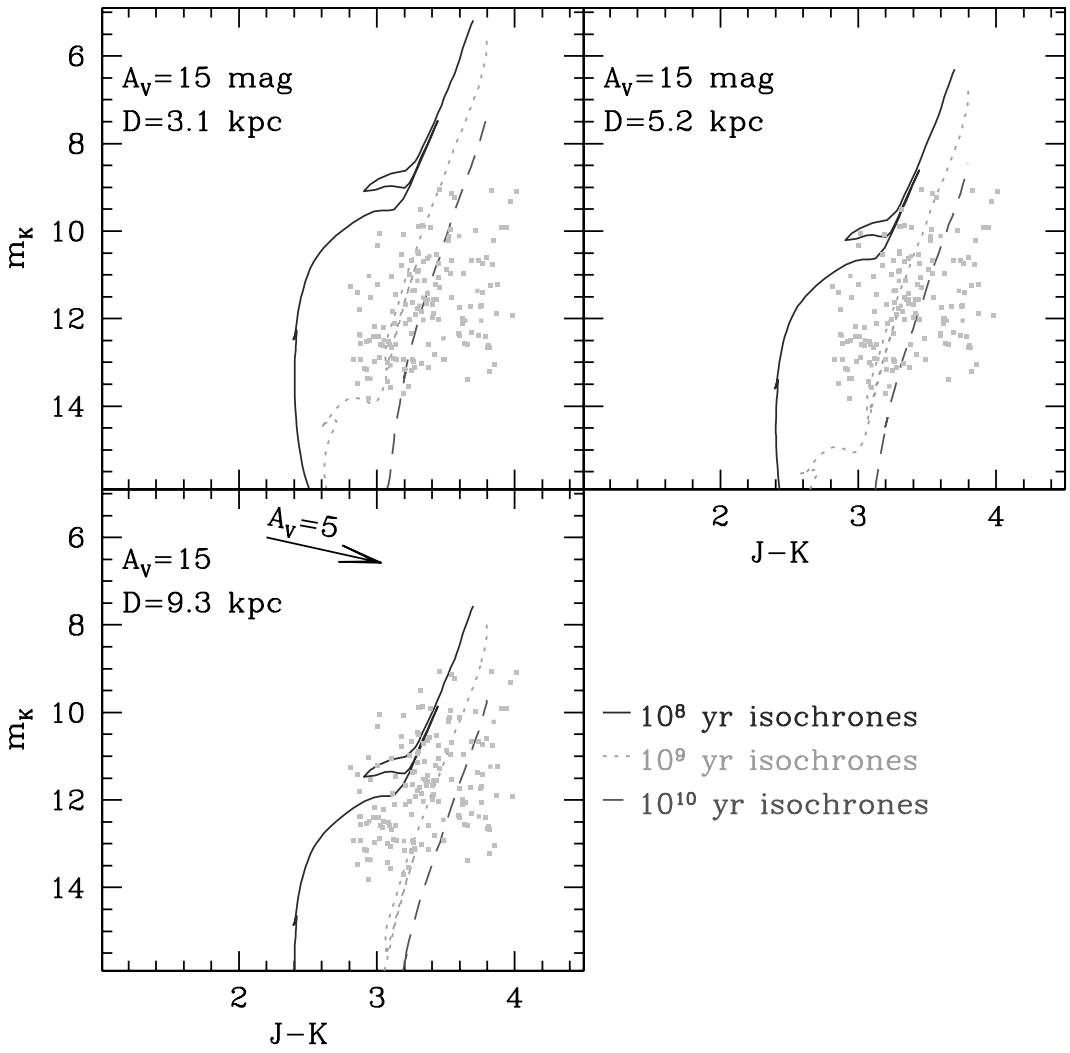

FIG. 7.—The K vs. $J-K$ CMD of stars within 45″ of the cluster center from within the dotted box in Fig. 6. Lines show the theoretical isochrones of Bonatto et al. (2004) for ages of 10^8 yr (*solid*), 10^9 yr (*dotted*), and 10^{10} yr (*dashed*). The three panels compare the isochrones with WIRO photometry for distances of 3.1, 5.2, and 9.3 kpc. The best fit is achieved with the 10^9 or 10^{10} yr isochrones at a distance of 3.1–5.2 kpc, consistent with the kinematic ^{13}CO distance.

star clusters'' found in nearby starburst galaxies (reviewed by Whitmore 2000) but would be extraordinary for a globular cluster.

3.5. *Cluster Properties*

Figure 9 illustrates how the derived physical properties of GLIMPSE-SC01 scale with distance. The shaded region highlights the most probable distance. The top two panels show that the inferred K-band and V-band luminosities are $M_K = -10.3$ and $M_V = -8.4$ for distances near 3.1 kpc. For the larger but less probable distances, these luminosities would be correspondingly larger. Here, the V-band luminosities have been derived from the measured K-band luminosities using the theoretical colors, $V - K = 1.9$, for a instantaneous burst stellar population with an age of 10^9–10^{10} yr (Leitherer et al. 1999). The mass of the cluster in the third panel is inferred from the theoretical mass-to-light ratio (tabulated by Bonatto et al. 2004) for three different representative ages of 10^8, 10^9, and 10^{10} yr. In any case, the mass of the cluster exceeds $10^5\ M_\odot$ for all reasonable distances and surpasses $10^6\ M_\odot$ if the age is very old or the distance is large. The conservative mass estimate of $10^5\ M_\odot$ is similar to Galactic globular clusters and young super star clusters with measured dynamical masses in nearby starbursts (e.g., NGC 1569; Ho & Filippenko 1996). The bottom panel of Figure 9 indicates that the half-light diameter of the cluster falls in the range 1–2 pc. This is smaller than most globular clusters, which have half-light diameters of 3–6 pc (Harris 1996). It is possible that the passage of GLIMPSE-C01 through the Galactic disk or a prolonged presence near the disk has stripped some fraction of the outer, loosely bound cluster members and left only the tightly bound cluster core.

4. DISCUSSION OF WHY GLIMPSE-C01 IS LIKELY TO BE A GLOBULAR CLUSTER

Several lines of evidence, as follows, favor identifying GLIMPSE-C01 as a member of the classical Milky Way globular cluster system rather than a young stellar cluster or even an evolved old open cluster.

Lack of radio emission.—Prominent Galactic star formation regions are luminous thermal radio and infrared sources with fluxes of many tens or even hundreds of janskys (e.g., Westerlund 2/RCW49; Churchwell et al. 2004). A modest star-forming region like Orion has an integrated 1420 GHz flux of 420 Jy at a distance of 450 pc (Felli et al. 1993). Orion would have a radio continuum flux of 9.4 Jy at 3.1 kpc, the adopted distance of GLIMPSE-C01, or a flux of 225 mJy, if it were on the far rim of the Galaxy. The new cluster, by comparison, is a

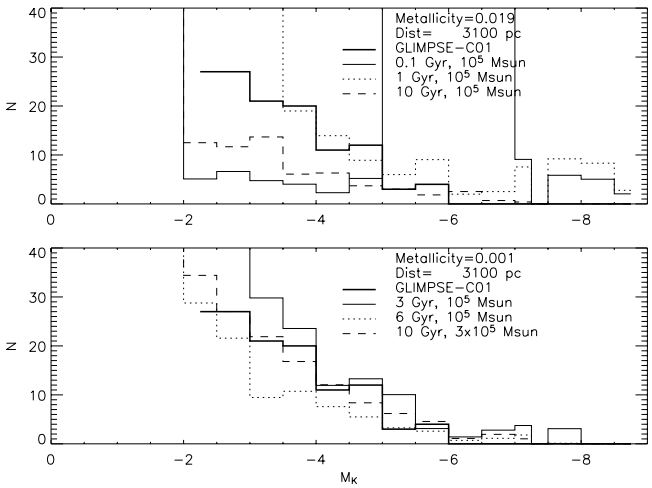

FIG. 8.—The *K*-band luminosity function of GLIMPSE-C01 (*thick line*) compared with theoretical luminosity functions from the Bonatto et al. (2004) isochrones for a cluster mass of $10^5\ M_\odot$, a distance of 3.1 kpc, and three different ages. The *K*-band data have been corrected for 1.7 mag of extinction ($A_V = 15$). The top panel shows luminosity functions for $Z = 0.019$ (approximately solar metallicity) clusters with ages of 10^8, 10^9, and 10^{10} yr. The bottom panel shows luminosity functions for $Z = 0.001$ (approximately $\frac{1}{20}$ solar metallicity) clusters with ages of 3×10^9, 6×10^9, and 10^{10} yr. Clusters of any metallicity with ages $\leq$3 Gyr are inconsistent with the observed luminosity function because of the lack of supergiants with luminosities $M_K < -6$ in GLIMPSE-C01.

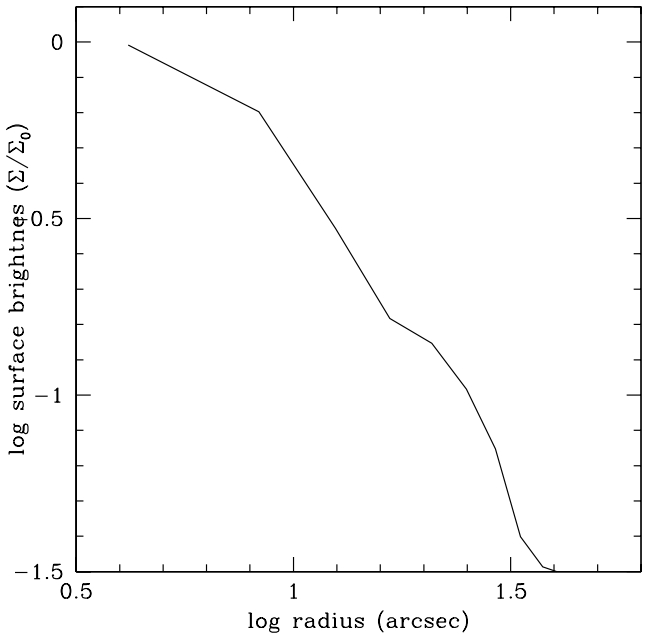

FIG. 10.—The 3.6 μm surface brightness as a function of radius for GLIMPSE-C01, normalized to the central surface brightness. At large radii the surface brightness becomes very uncertain because of contamination by field stars in the Galactic plane.

marginal detection at less than 5 mJy in the radio continuum, indicating that no massive stars are present. The lack of radio synchrotron sources or diffuse infrared shells suggests that we can rule out recent supernova remnants.

A well-populated giant branch.—Given the infrared photometry presented in Figure 6 and the *K*-band luminosity function in Figure 8, the cluster contains a wealth of giant stars but a lack of luminous supergiants, consistent with the evolved nature of a globular cluster. Preliminary *K*-band spectroscopy of GLIMPSE-C01 shows no emission lines that should be present in a very young OB-type cluster (Clemens 2005).

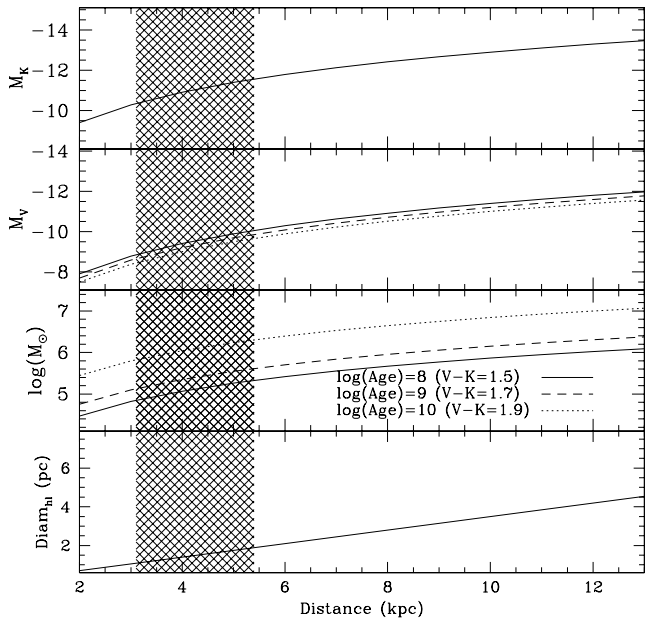

FIG. 9.—Cluster properties vs. assumed distance. The most probable distances between 3.1 and 5.2 kpc are shaded. The *V*-band luminosity ranges between $M_V = -8.4$ and -10.0 for plausible distances. The total mass is 10^5–$10^6\ M_\odot$ for the most probable ages and distances.

Overall luminosity.—With an absolute *V* magnitude estimated at $M_V = -8.4$, the cluster is more luminous than the majority of known globular clusters (Harris 1996) and vastly more luminous and massive than known old open clusters, even at the conservative distance of 3.1 kpc.

Stellar density.—GLIMPSE-C01 is a rich, centrally condensed cluster with evidence for mass segregation characteristic of dynamically relaxed systems. Figure 10 shows the 3.6 μm surface brightness as a function of radius, normalized to the central surface brightness. At large radii the surface brightness becomes very uncertain as a result of contamination by field stars. Open clusters, in general, do not survive long enough to become dynamically relaxed. Figure 11 compares the IRAC 4.5 μm image of GLIMPSE-C01 (*left*) with the 2MASS *K*-band image of the old open cluster NGC 6791 (*right*), which lies at a similar distance (4 kpc). NGC 6791 is $\sim$7 Gyr old (Demarque et al. 1992) but not as rich or centrally condensed as the new cluster, even though it is at a similar distance (4.0 kpc).

Position in the Galaxy.—At $\leq$6.1 kpc from the Galactic center, GLIMPSE-C01 is interior to known old (>1 Gyr) open clusters, which are only found at $R_{GC} > 7.5$ kpc (Friel 1995). Survival over gigayear timescales requires that a weakly bound old open cluster be protected from disruption by the gravitational forces of giant molecular clouds and stellar encounters, which are more prevalent inside the solar circle. Globular clusters, on the other hand, are preferentially found toward the Galactic bulge.

Given the evidence, it appears likely that GLIMPSE-C01 is a massive globular cluster making a passage through the Galactic disk. The morphology of the cluster and surrounding ISM, if physically associated with the cluster, may provide some clues regarding its trajectory.

The outer isophotes of GLIMPSE-C01 are significantly elliptical, having $e = (1 - b/a) = 0.21$ at 72″ from the nucleus. Figure 12 shows the IRAC 3.6 μm image with a series of best-fit

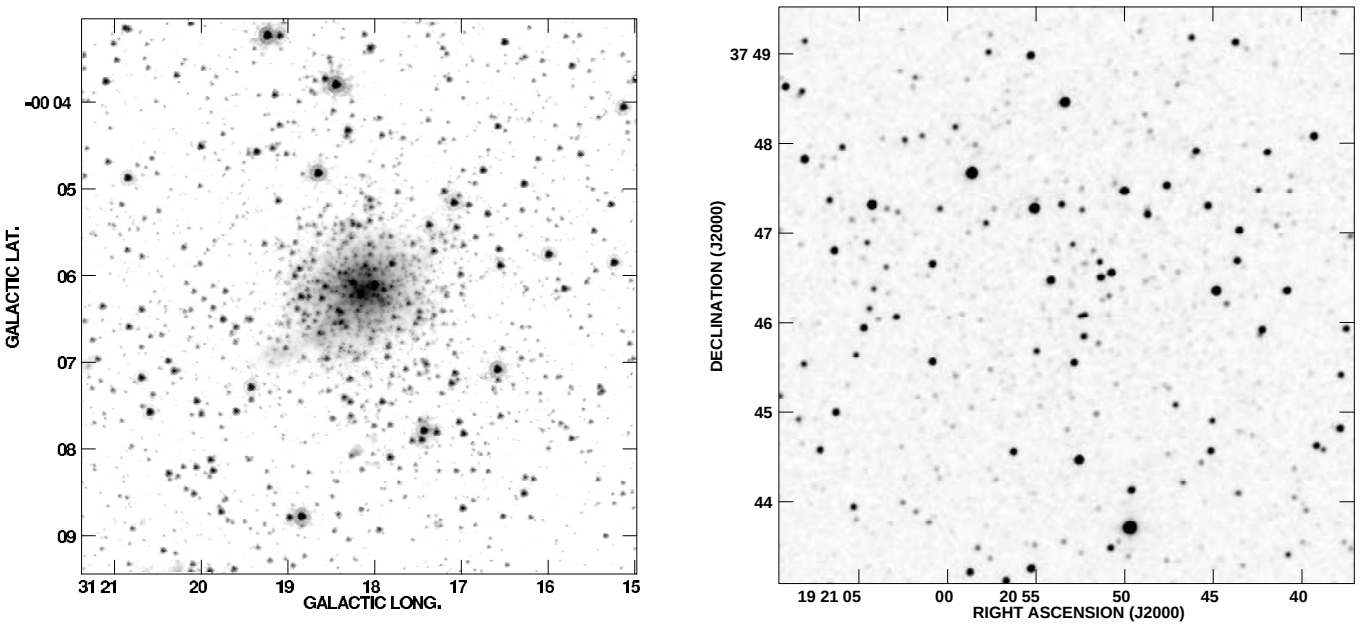

FIG. 11.—Comparison of the richness of the putative globular cluster GLIMPSE-C01 seen at 4.5 μm to the old open cluster NGC 6791 ($D = 4$ kpc) from the 2MASS K' image (*right*).

ellipses having semimajor axes of 12″, 24″, 36″, 48″, 60″, and 72″. The ellipticity of the outer ellipses shows that the major axis of the cluster lies along a position angle (P.A.) of 124° in Galactic coordinates, or 61° in J2000 equatorial coordinates.

The bright plume of PAH emission seen in Figure 2 lies at the same P.A. as the major axis of the cluster's outer isophotes, suggesting a preferred orientation at a P.A. of ∼124° from Galactic north (P.A. = 61° in equatorial coordinates). One end of the plume is centered on the cluster, and the other end extends 1.′5 to the Galactic south of the cluster and toward higher longitudes. One possibility is that the plume traces intracluster or circumstellar debris from GLIMPSE-C01, which has been stripped by the Galactic ISM as the cluster moves from south to north across the plane. An alternative scenario is that the diffuse ribbon of emission extending to the Galactic north and toward lower longitudes traces the recent trajectory of the cluster and

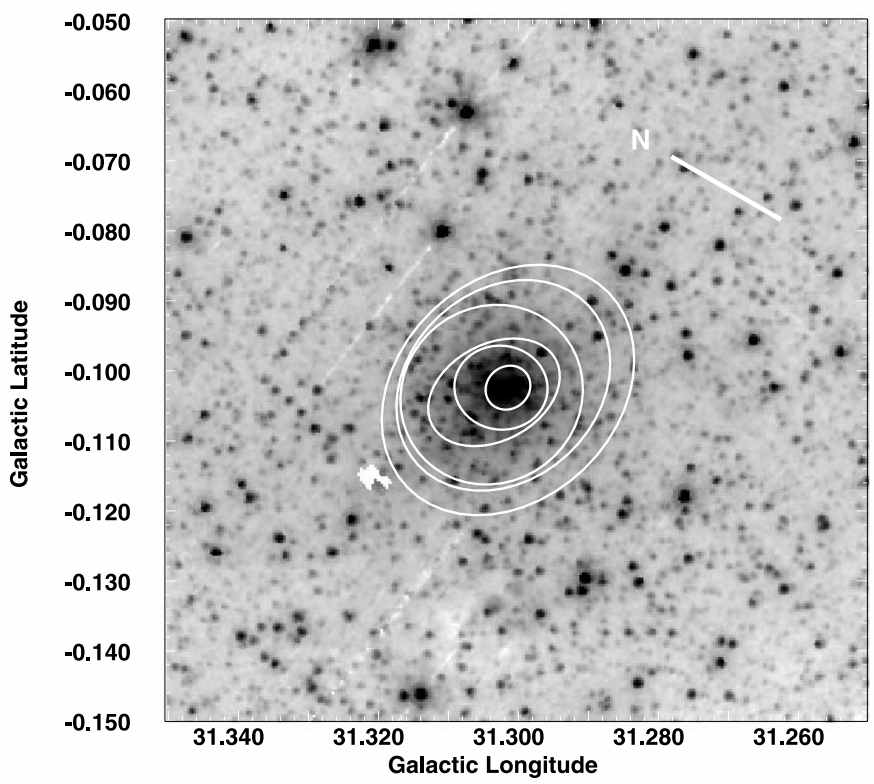

FIG. 12.—IRAC 3.6 μm image of GLIMPSE-C01 with a series of best-fit ellipses, with semimajor axes of 12″, 24″, 36″, 48″, 60″, and 72″. The line labeled "N" designates north in equatorial coordinates. The outer two ellipses show that the cluster is elongated, with ellipticity $e = 1 - (b/a) = 0.2$ at P.A. of 124° in Galactic coordinates (61° in J2000 equatorial coordinates).

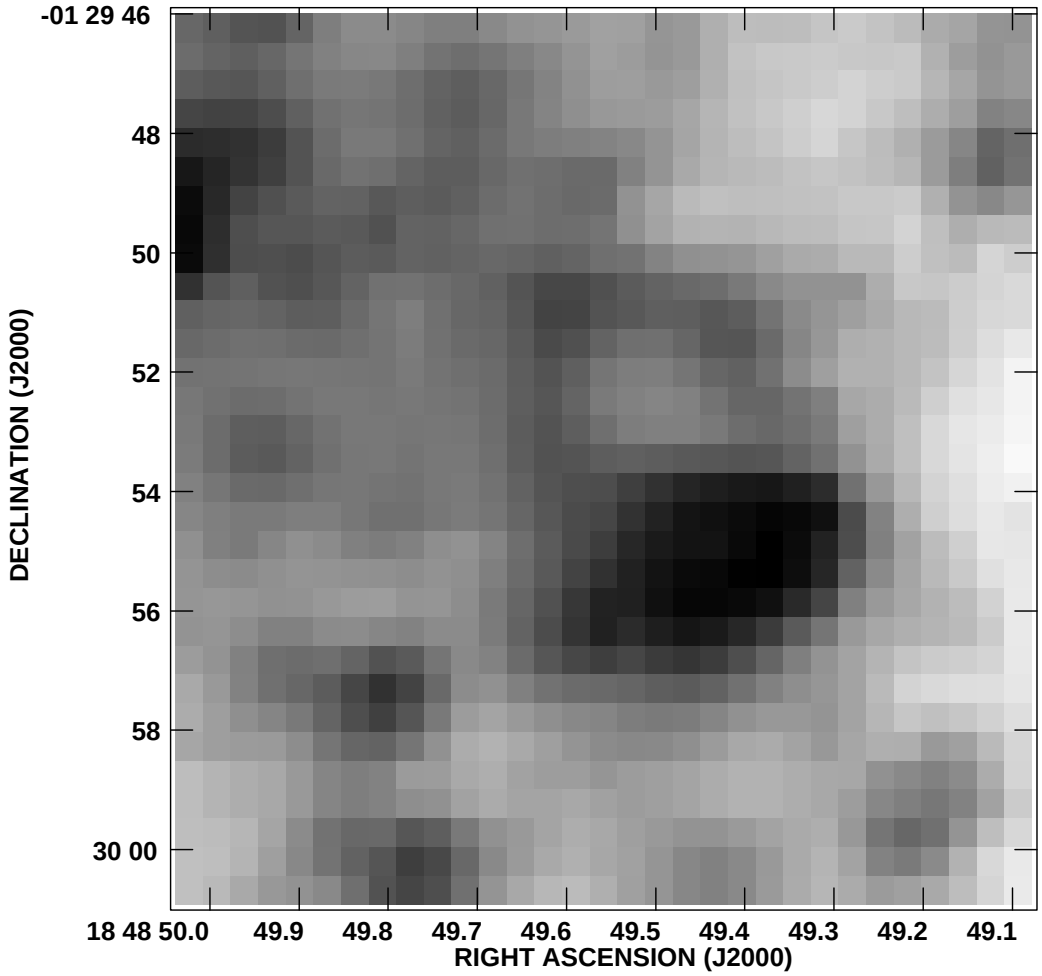

FIG. 13.—Subsection of the WIRO *H*-band image of the GLIMPSE-C01 showing a looplike structure that is seen at all near- and mid-infrared continuum bands. The loop has a diameter of about 9 pixels, corresponding to a linear diameter of 0.058 pc or ~12,000 AU at 3.1 kpc. This object may be an old nova shell or a young planetary nebula.

that the plume is caused by recent star formation as the cluster impacts the Galactic molecular layer on its journey to the south. The possibility remains, of course, that the diffuse IR emission lies in the foreground or background and is not affiliated with the cluster.

One interesting object visible in both the WIRO near-IR and IRAC mid-IR images is a looplike structure on the Galactic north side of the brightest stellar peak in the cluster. The center of the loop is located at R.A. (J2000) = $18^{h}48^{m}49^{s}.58$, decl. (J2000) = $-01^{\circ}29'53''$. Figure 13 shows the WIRO *H*-band image of a small region around this feature. The loop has a diameter of about 9 pixels ($4''$) in the WIRO images. It is seen at all wavelengths, except 8 μm where the angular resolution of *Spitzer*/IRAC becomes insufficient to resolve it. At the adopted distance of the cluster, the linear diameter of the loop would be 0.058 pc, or ~12,000 AU. This size is much larger than dust shells ejected by individual asymptotic giant branch stars near the end of their lives. The lack of strong radio emission rules out a supernova remnant. The shell diameter is comparable to the dimensions of old nova shells with ages of tens of years (e.g., Downes & Duerbeck 2000), which are generally seen in emission lines but sometimes detected in continuum light. Dust in the shell could scatter stellar light from the cluster and explain the strong continuum detection. The object may also be a young planetary nebula shell. In either case, velocity-resolved spectroscopy should be performed to measure the kinematics of the shell and provide additional clues to its origin. If the object is a recent nova shell produced by a cluster member and if archival images exist that could pinpoint the date of the nova, then a measured expansion velocity could be used to measure a direct kinematic distance to the cluster, independent of assumptions about a Galactic rotation curve or peculiar cluster motions. However, with optical extinctions of $A_V = 15$, even the brightest Galactic novae with absolute visual magnitudes of -11 (Duerbeck 1981) would only reach apparent magnitudes of $V = 16$, making it unlikely that it would have been observed. If the object is a planetary nebula, chemical analysis of the nebula would help to determine whether GLIMPSE-C01 belongs to the older, metal-poor halo population of globular clusters or the younger, more metal-rich disk population.

This discovery of a new nearby globular cluster suggests a plethora of follow-up observational programs. High-resolution IR spectroscopy of cluster members would be highly desirable to estimate its radial velocity and establish a kinematic distance. A proper-motion measurement is needed to compute its orbital parameters and determine a probable origin in either the old halo cluster population of the younger disk population. Deep wide-field IR photometry would help to establish the boundaries of the cluster and better constrain its total luminosity. The region of Y-shaped stellar outflows to the south (Galactic) of the cluster will make an interesting target for multiwavelength studies of star formation activity in the vicinity of the cluster.

Note added in manuscript.—As this paper went to press, we became aware of a previous identification of the GLIMPSE-C01 cluster by Simpson & Cotera (2004) using 2MASS near-infrared images to identify *ASCA* X-ray and *IRAS* sources in the Galactic plane. They state that the new cluster has the appearance of a globular cluster in 2MASS images.

We thank the anonymous referee for a timely and helpful review. We are grateful to Stephan Jansen for his invaluable work maintaining the GLIMPSE computing network. We thank Jim Weger and Phil Haynes for assistance at WIRO. We thank Ata Sarajedini for suggesting analysis of the *K*-band luminosity function, which led to a more robust distance and age estimate. Support for this work, part of the *Spitzer* Space Telescope Legacy Science Program, was provided by the National Aeronautics and Space Administration (NASA) through contract numbers (institutions) 1224653 (Univ. Wisconsin–Madison), 1225025 (Boston Univ.), 1224681 (Univ. Maryland), 1224988 (Space Sci. Inst.), 1259516 (Univ. California, Berkeley), 1253153 (Univ. Minnesota), 1253604 (Univ. Wyoming), 1256801 (Univ. Wisconsin–Whitewater) by the Jet Propulsion Laboratory, California Institute of Technology (Caltech) under NASA contract 1407. B. U. was supported by a Wyoming NASA Space Grant Consortium, NASA grant NGT-40102 40102, Wyoming NASA EPSCoR grant NCC5-578 and 1253604. This publication makes use of data products from the Two Micron All Sky Survey, which is a joint project of the University of Massachusetts and the Infrared Processing and Analysis Center (IPAC)/Caltech, funded by the NASA and the National Science Foundation (NSF). The Two Micron All Sky Survey is a joint project of the University of Massachusetts and the IPAC/Caltech, funded by NASA and the NSF.

REFERENCES

Benjamin, R., et al. 2003, PASP, 115, 953
Bica, E., Dutra, C. M., Soares, J., & Barbuy, B. 2003, A&A, 404, 223
Bohlin, R. C., Savage, B. D., & Drake, J. F. 1978, ApJ, 224, 132
Bonatto, C., Bica, E., & Girardi, L. 2004, A&A, 415, 571
Borissova, J., Pessev, P., Ivanov, V. D., Saviane, I., Kurtev, R., & Ivanov, G. R. 2003, A&A, 411, 83
Cardelli, J. A., Clayton, G. C., & Mathis, J. S. 1989, ApJ, 345, 245
Carpenter, J. 2001, AJ, 121, 2851
Churchwell, E. B., et al. 2004, ApJS, 154, 322
Clemens, D. P. 1985, ApJ, 295, 422
———. 2005, in preparation
Condon, J. J., Cotton, W. D., Greisen, E. W., Yin, Q. F., Perley, R. A., Taylor, G. B., & Broderick, J. J. 1998, AJ, 115, 1693
Demarque, P., Guenther, D. P., & Green, E. M. 1992, AJ, 103, 151
Downes, R. A., & Duerbeck, H. W. 2000, AJ, 120, 2007
Duerbeck, H. W. 1981, PASP, 93, 165
Dutra, C. M., Bica, E., Soares, J., & Barbuy, B. 2003, A&A, 400, 533
Fazio, G., et al. 2004, ApJS, 154, 10
Felli, M., Churchwell, E., Wilson, T. L., & Taylor, G. B. 1993, A&AS, 98, 137
Friel, E. D. 1995, ARA&A, 33, 381
Harris, W. E. 1996, AJ, 112, 1487
Hawarden, T. G., Leggett, S. K., Letawsky, M. B., Ballantyne, D. R., & Casali, M. M. 2001, MNRAS, 325, 563
Ho, L., & Filippenko, A. V. 1996, ApJ, 466, L83
Hurt, R. L., Jarrett, T. H., Kirkpatrick, J. D., Cutri, R. M., Schneider, S. E., Skrutskie, M., & van Driel, W. 2000, AJ, 120, 1876
Indebetouw, R., et al. 2005, ApJ, in press
Langer, W. D., & Penzias, A. A. 1990, ApJ, 357, 477
Leitherer, C., et al. 1999, ApJS, 123, 3
Maloney, P. R., & Black, J. H. 1988, ApJ, 325, 389
Mercer, E. P., et al. 2004, ApJS, 154, 328
Richardson, K. M., & Wolfendale, A. W. 1988, A&A, 201, 100
Schlegel, D. J., Finkbeiner, D. P., & Davis, M. 1998, ApJ, 500, 525
Simon, R., Jackson, J. M., Clemens, D. P., Bania, T. M., & Heyer, M. H. 2001, ApJ, 551, 747
Simpson, J. P., & Cotera, A. S. 2004, BAAS, 204, No. 45.01
Whitmore, B. A. 2000, in STScI Symp. Ser. 14, A Decade of *HST* Science, ed. M. Livio (Baltimore: STScI), 153
Whitney, B. A., et al. 2004, ApJS, 154, 315